# Miscibility and Thermal Behavior of Poly(vinyl chloride)/Feather Keratin Blends

**Shahin Akhlaghi,[1] Alireza Sharif,[1,2] Mohammadreza Kalaee,[1] Mohammadreza Manafi[3]**

[1]Department of Polymer Engineering, Islamic Azad University, Tehran South Branch, Tehran, Iran
[2]Department of Polymer Science and Technology, Research Institute of Petroleum Industry, Tehran, Iran
[3]Department of Applied Chemistry, Islamic Azad University, Tehran South Branch, Tehran, Iran

**ABSTRACT:** Various poly(vinyl chloride) (PVC)/feather keratin (FK) blends were prepared via a solution blending method in the presence of *N,N*-dimethylformamide as a solvent. The miscibility of the blends was studied with different analytical methods, such as dilute solution viscometry, differential scanning calorimetry, refractometry, and atomic force microscopy. According to the results obtained from these techniques, it was concluded that the PVC/FK blend was miscible in all the studied compositions. Specific interactions between carbonyl groups of the FK structure and hydrogen from the chlorine-containing carbon of the PVC were found to be responsible for the observed miscibility on the basis of Fourier transform infrared spectroscopy. Furthermore, increasing the FK content in the blends resulted in their miscibility enhancement. The thermal stability of the samples, as an important characteristic of biobased polymer blends, was finally examined in terms of their FK weight percentage and application temperature. © 2011 Wiley Periodicals, Inc. J Appl Polym Sci 121: 3252–3261, 2011

**Key words:** miscibility; polymer blends; poly(vinyl chloride) (PVC); solution properties; thermal properties

## INTRODUCTION

Concerns over environmental impacts, such as global warming, pollution, and use of renewable versus nonrenewable resources, and the cost of synthetic polymers have recently motivated significant research in support of sustainable polymer systems in which one or more component is biodegradable or biobased.[1,2] Among the existing biopolymers resources, feather keratin (FK) is one of the most abundant and inexpensive polymers; it possesses unique properties, such as a high aspect ratio and good thermal and acoustic insulating characteristics.[3] According to global statistics, feather waste production in the world amounts to more than 4 million tons annually; this disposal presents a severe problem for the poultry industry.[4] Several approaches are in vogue for disposing of bulk feather waste, including landfilling, burning, natural gas production, and treatment for animal feed;[5,6] these are all environmentally unsound and, therefore, undesirable in a tide of increasingly restrictive environmental regulations.[7] With regard to the aforementioned difficulties, using these wastes as potential substitutes for synthetic polymers provides an ecofriendly alternative to their disposal methods.

Nevertheless, FK by itself has serious limitations because of its poor mechanical properties and brittleness compared to those of synthetic polymers.[8,9] To overcome these deficiencies, many attempts have been directed toward modification of the FK chemical structure.[8–12] For example, Schrooyen et al.[9] found that a controlled interaction of cysteine residues of the FK structure with iodoacetic acid not only provided more stable FK solutions for film casting but also left the remaining cysteines free to form disulfide crosslinks during film formation; this, in turn, resulted in enhanced mechanical properties of the modified FK. Moreover, Tanabe et al.[10] reported that the keratin films crosslinked by ethylene glycol diglycidyl ether had a higher mechanical strength and elongation at break compared to pure keratin films.

Another approach in this regard, however, is FK blending with other synthetic polymers. The resultant blends would be more environmentally friendly than completely synthetic products because of the biodegradation properties provided by FK. Furthermore, synthetic polymers/FK blends would have superior mechanical properties compared to products developed solely from FK.

In recent years, many research works have been devoted to the study of the blends and composites of synthetic polymers and FK. For instance, Barone and Schmidt[13,14] studied various polyethylene-based

composites containing keratin fibers from chicken feathers. The results showed that the elastic modulus and yield stress of the composites increased over those of the virgin polymer. Also, Huda and Yang[15] reported that composites from ground chicken quill and polypropylene had superior flexural moduli, tensile properties, and noise reduction coefficients compared to polypropylene/jute composites because of the significantly lower aspect ratio and length of ground quill over jute. In addition, Martinez-Hernandez et al.[16] observed that the thermal stability, glass-transition temperature ($T_g$), and storage modulus of poly(methyl methacrylate) increased with chicken feather fibers addition. Recently, Cheng et al.[17] studied chicken feather fiber/poly(lactic acid) green composites and noticed that the storage modulus of the composites increased and the mechanical loss factor decreased with respect to the pure polymer. Moreover, Mishra et al.[18] studied epoxy- and alkali-treated FK composites and showed that the composites' tensile and flexural strengths were enhanced over the pure epoxy resin. Furthermore, Barone and Gregoire[19] characterized fiber/polymer interactions in short keratin fiber/polypropylene composite. They pointed out increased interaction between polypropylene and FK fibers as a result of a coupling agent, maleic anhydride grafted polypropylene, introduced to the composites. The interaction enhancement and the resultant mechanical properties improvement was attributed to a distinct increase in the amount of transcrystallinity in the composites.

Nevertheless, even though the miscibility of the blend constituents plays a vital role in the manifestation of superior properties of a blend at the molecular scale, one can acknowledge that investigations concerning synthetic polymer/FK miscibility are lacking in the open literature. A fundamental understanding of the extent of the miscibility between the FK and synthetic polymers would enhance the capability for modifying the properties of this natural polymer by its blending with other polymers.

Therefore, this work is concerned with the examination of the miscibility of poly(vinyl chloride) (PVC), one of the most consumed plastics in the world, with FK with various techniques. To do so, various PVC/FK mixtures were prepared by a solution blending method. Dilute solution viscometry (DSV), Fourier transform infrared (FTIR) spectroscopy, differential scanning calorimetry (DSC), refractometry, and atomic force microscopy (AFM) were used to gather the miscibility data. When these data were analyzed, the PVC/FK blend could be referred to as miscible if the blend components formed a homogeneous single-phase mixture.[20] In addition, the thermal stability of the prepared blends was studied with thermogravimetric analysis (TGA).

## EXPERIMENTAL

### Materials

PVC, with a $k$-value (a measure of molecular weight) of 65, was obtained from Bandar Imam Petrochemical Co. (Mahshahr, Iran). Poultry feather was purchased from Zarbal Co. (Amol, Iran). FK fibers, 3–4 cm in length, were manually cut from the feather shaft, thoroughly washed with ethanol, and then dried. Furthermore, $N,N$-dimethylformamide (DMF; Merck) was used as received.

### Sample preparation

Various PVC/FK blends were prepared via a solution blending method. At first, each of the blend components was dissolved separately in its common solvent, DMF, to create master solutions. It should be noted that a homogeneous solution of the FK in DMF was obtained by continuous stirring of the FK/DMF mixture at 80°C for 5 days. Then, the master solutions were mixed together in such ratios that various mixtures with 20, 40, 50, and 60 wt % FK were obtained. Finally, the mixed solutions were cast on Petri dishes, and the solvent was removed by evaporation in a vacuum oven at 80°C for 48 h. The resultant PVC/FK blend films, about 90 μm in thickness, were used for later analysis.

### Characterization methods

#### DSV

*Equations of the blend viscosity versus concentration.* The viscosities of the parent polymer and blend dilute solutions in DMF were measured with an Ubbelohde capillary viscometer (Schott, Mainz, Germany) immersed in a constant-temperature bath at 25.0 ± 0.1°C. According to Krigbaum and Wall[21] and Cragg and Bigelow,[22] the reduced viscosity of a polymer ($\eta_{sp}/C$) in a solution follows the Huggins equation:

$$(\eta_{sp}/C)_i = [\eta]_i + b_{ii}C_i \qquad (1)$$

where

$$b_{ii} = k_{ii}[\eta]_i^2 \qquad (2)$$

where $(\eta_{sp})_i$, $\eta_i$, $C_i$, $b_{ii}$, and $k_{ii}$ are the specific viscosity, intrinsic viscosity, polymer concentration, viscometric interaction parameter, and Huggins constant of polymer $i$, respectively. For nonelectrolyte dilute solutions, a plot of $(\eta_{sp}/C)_i$ versus $C_i$ should yield a straight line with intercept and slope equal to $\eta_i$ and $b_{ii}$, respectively. Theoretically, the parameter $\eta_i$ measures the effective hydrodynamic specific volume of a single polymer, whereas the quantity $b_{ii}$ returns to the binary interactions between polymer

segments.[20] Equation (1) can be readily adapted to a ternary system containing a polymer (1), a polymer (2), and a solvent (3), as follows:[20]

$$(\eta_{\rm sp}/C)_m = [\eta]_m + b_m C_m \tag{3}$$

by setting

$$b_m = b_{11}w_1^2 + b_{22}w_2^2 + 2b_{12}w_1w_2 \tag{4}$$

where $[\eta]_m$ and $b_m$ is the experimental intrinsic viscosity and viscometric interaction parameter of a ternary solution, $C_m$ is the total concentration of polymers 1 and 2 ($C_m = C_1 + C_2$), and $w_i$ designates the normalized weight fraction of polymer $i$ (i.e., $w_i = C_i/C_m$, where $i = 1$ and 2). Also, $b_{12}$ is the experimental viscometric interaction parameter between the two polymeric species.

*Criteria of blend miscibility.* According to Williamson and Wright,[23] in blends with ideal behavior, the interspecific interaction coefficient ($b_{12}^{id}$) can be expressed as

$$b_{12}^{id} = (b_{11} + b_{22})/2 \tag{5}$$

According to this approach, intermolecular interactions between two polymers can be evaluated on the basis of the difference between the experimental ($b_{12}$) and theoretical ($b_{12}^{id}$) values of the interaction parameter:

$$\Delta b = b_{12} - b_{12}^{id} \tag{6}$$

The values of $b_{12}$ and $b_{12}^{id}$ are obtained from a combination of eqs. (1)–(4) and Eq. (5), respectively. If $\Delta b \geq 0$ or $b_{12} \geq b_{12}^{id}$, there exist attractive intermolecular interactions and miscibility in the system, whereas $\Delta b \leq 0$ or $b_{12} \leq b_{12}^{id}$ implies the tendency of the system to go toward phase separation.

Using these values, Chee[24] introduced another parameter ($\mu$) to predict polymer–polymer miscibility, as follows:

$$\mu = \Delta b / ([\eta]_1 - [\eta]_2)^2 \tag{7}$$

where $\mu \geq 0$ indicates blend miscibility and $\mu < 0$ indicates immiscibility. Garcia et al.[25] also proposed a miscibility criterion, which was based on the difference between $\eta_m$ and the ideal value of the solution intrinsic viscosity ($[\eta]_m^{id}$):

$$\Delta[\eta] = [\eta]_m - [\eta]_m^{id} \tag{8}$$

where

$$[\eta]_m^{id} = [\eta]_1 w_1 + [\eta]_2 w_2 \tag{9}$$

The value of $[\eta]_m$ is determined from the intercept of the plot according to Eq. (3), whereas $[\eta]_m^{id}$ is calculated from Eq. (9). When $\Delta[\eta] < 0$, then the two polymers are miscible.

## FTIR measurements

The infrared spectra were acquired with a Bruker Equinox55 FTIR spectrophotometer (Karlsruhe, Germany) equipped with deuterated triglycine sulfate detector. The scans were taken at 4-cm$^{-1}$ resolution. All of the blend films were sufficiently thin to be within a range where the Beer–Lambert law is obeyed.

## Refractometry measurements

Refractive indices of the blend solutions were measured with an Abbe's refractometer (Erma Optical Words Ltd., Tokyo, Japan) with a thermostat water-circulation system at 30°C. The accuracy of the refractive index measurements was ±0.02%.

## DSC measurements

DSC measurements were performed on a Polymer Laboratory PL–DSC instrument (Church Stretton, England). The temperature was ramped at 10°C/min from 30 to 350°C under a nitrogen atmosphere. $T_g$ was determined by the intersection method, and the melting temperature ($T_m$) was taken as the maximum in the endothermic peak. Also, the heat of fusion per gram of sample ($\Delta H_f$) was determined by measurement of the melting peak area for each sample.

## TGA measurements

The TGA curves were recorded on a Polymer Laboratories TGA–Polymer Laboratory PL instrument (Church Stretton, England). All the experiments were carried out at a heating rate of 10°C/min from 30 to 600°C under a nitrogen atmosphere.

## AFM

Tapping-mode AFM was performed with a Dualscope/Rasterscope C26 Danish Micro Engineering (DME) with alternating Current (AC) (Copenhagen, Denmark) probe equipped with an aluminum coating cantilever. All measurements were made at ambient temperature, and intermediate to hard tapping was employed to reveal good contrast in both height and phase images.
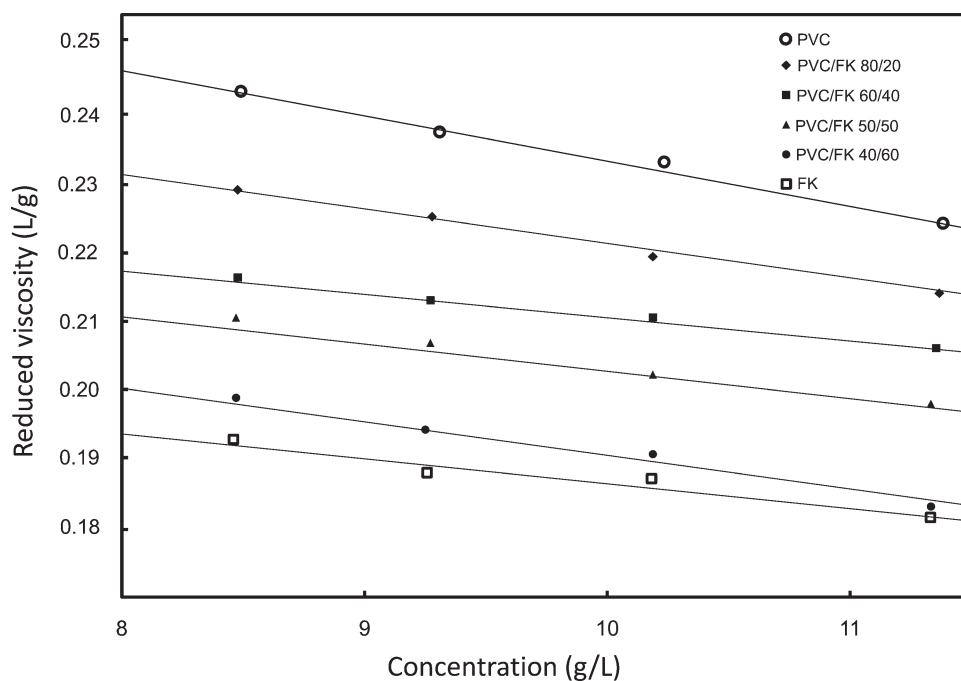
**Figure 1** $\eta_{sp}/C$ versus concentration for the pure PVC, FK, and various PVC/FK solutions.

## RESULTS AND DISCUSSION

Figure 1 illustrates the variation of $\eta_{sp}/C$ of the parent polymers and various PVC/FK blend solutions as a function of their concentrations. A linear relationship was observed for all of the blends over the studied composition range. The values of $b_m$ and $\eta_m$ were attained from the slopes and intercepts of the experimental lines in Figure 1, respectively. As can be seen, the blends' $\eta_m$ values increased with increasing PVC content; this could be interpreted by the higher $\eta_m$ value of neat PVC over that of the pure FK. Accordingly, the values of $\Delta b$ and $\mu$ were computed with eqs. (6) and (7) and are given in Table I.

It should be noted that the values of $b_{11}$ and $b_{22}$ were derived from the $\eta_{sp}/C$ versus $C$ curves of pure FK and PVC (Fig. 1). As can be seen from Table I, the parameters $\Delta b$ and $\mu$ were positive. Hence, the PVC/FK blends could be classified as miscible at all the studied compositions on the basis of the criteria introduced previously in the Experimental section.

Moreover, in all the PVC/FK blends, $\eta_m$ values revealed a negative deviation from the mixing rule (Fig. 2). Therefore, according to the $\Delta[\eta]$ criterion proposed by Garcia, all the studied PVC/FK blends were miscible (Table I). Also, it can be seen from Table I that the system containing the highest FK weight percentage, PVC/FK 40/60, had the greatest deviation from the mixing rule. This observation may point to the fact that interaction between the blend components increased as the FK weight percentage increased. For the sake of clarity, the most abundant chemical structures that are found in FK are shown in Figure 3. Proline, serine, valine, cysteine, and glycine amino acids of FK can serve arrays of polar side groups, such as amino, hydroxyl, sulfhydryl, and carboxyl, which may act as potential sites for increasing its interactions with PVC chains. This finding runs in harmony with the conclusion derived by Lizymol and Thomas[26] and Walsh et al.,[27] who stated that blends of two components with different polarities show more compatibility when the fraction of the more polar component increases.

The FTIR spectra of solid FK, soluted FK, PVC, and PVC/FK 50/50 blend are shown in Figure 4. The most important spectral features in the 600–700-$cm^{-1}$ region were those of sulfur–sulfur (S—S) bonds
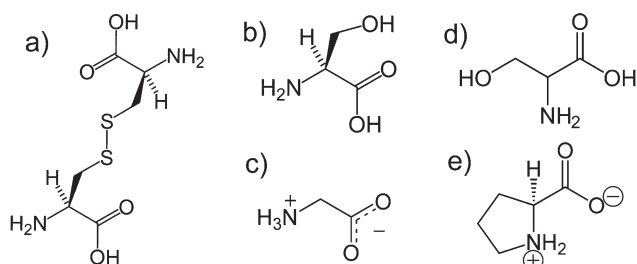
## TABLE I
### Compatibility Parameters for the Blends

| Sample | $\Delta b$ (L/g) | $\mu$ | $\Delta[\eta]$ (L/g) |
|---|---|---|---|
| PVC/FK 40/60 | 5.1555 ± 0.02 | 3.2725 ± 0.15 | −0.2491 ± 0.002 |
| PVC/FK 50/50 | 5.0176 ± 0.021 | 2.4630 ± 0.22 | −0.1848 ± 0.003 |
| PVC/FK 60/40 | 4.3154 ± 0.05 | 1.9946 ± 0.072 | −0.1172 ± 0.002 |
| PVC/FK 80/20 | 4.4628 ± 0.044 | 1.6957 ± 0.084 | −0.0699 ± 0.004 |
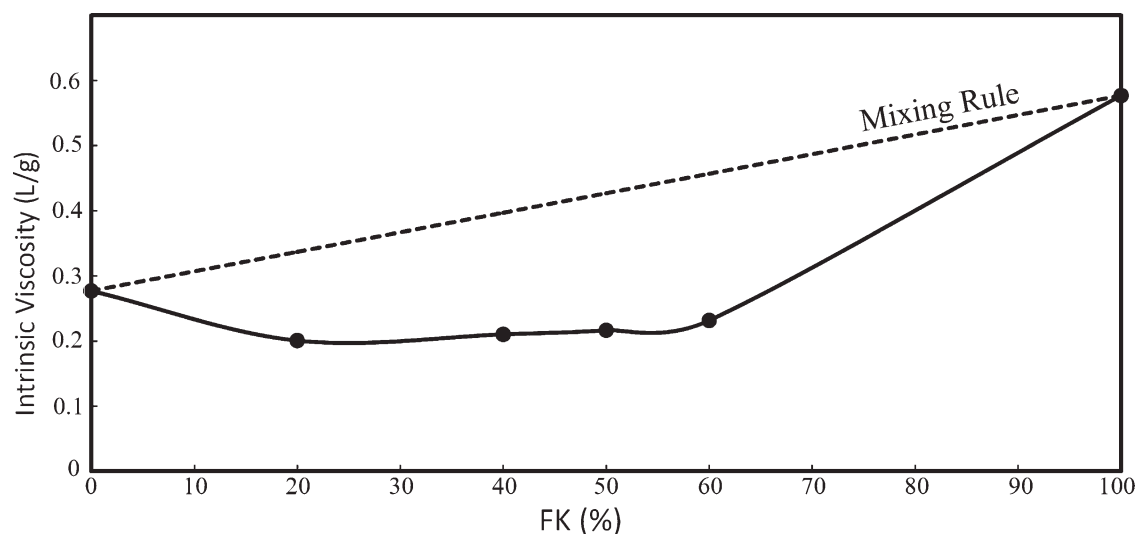
**Figure 2** Intrinsic viscosity versus weight fraction of FK in the samples: (- - -) prediction in accordance with the mixing rule and (●) experimental data.

in the solid FK. It has been reported that the FK stability in the solid state is typically due to the crosslinking produced by the formation of cysteine disulfide bonds.[28] Therefore, the reduction of the S—S peak intensity and the appearance of a new peak at 1238 cm$^{-1}$ corresponding to a symmetric $SO_2$ band[29] in the soluted FK FTIR spectrum compared to that of the solid FK indicated the disulfide linkages cleaving during the dissolving process. In other words, it seems that the FK was dissolved and formed a molecular dispersion in DMF. All the samples containing FK showed the same vibrational modes in the 3100–3500- and 1500–1550-cm$^{-1}$ ranges, which corresponded to the N—H bands of the FK amides I, II, and III.[30] In addition, the most intense bands in the 1550–1700-cm$^{-1}$ region could be assigned to the C=O stretching vibration of amide I.[29] There were no vibrational transitions in the C=O and N—H peak positions of the soluted FK compared to their original positions in the solid FK FTIR spectrum. This observation revealed that no chain scissioning occurred in the FK chains during the dissolving process in DMF. Also, the characteris-

tic absorption peaks of PVC emerged at 700–750 cm$^{-1}$ (corresponding to C—Cl stretching), 958 cm$^{-1}$ (related to C—C stretching vibrations), 1300–1400 cm$^{-1}$ (corresponding to C—H stretching of $CH_2$
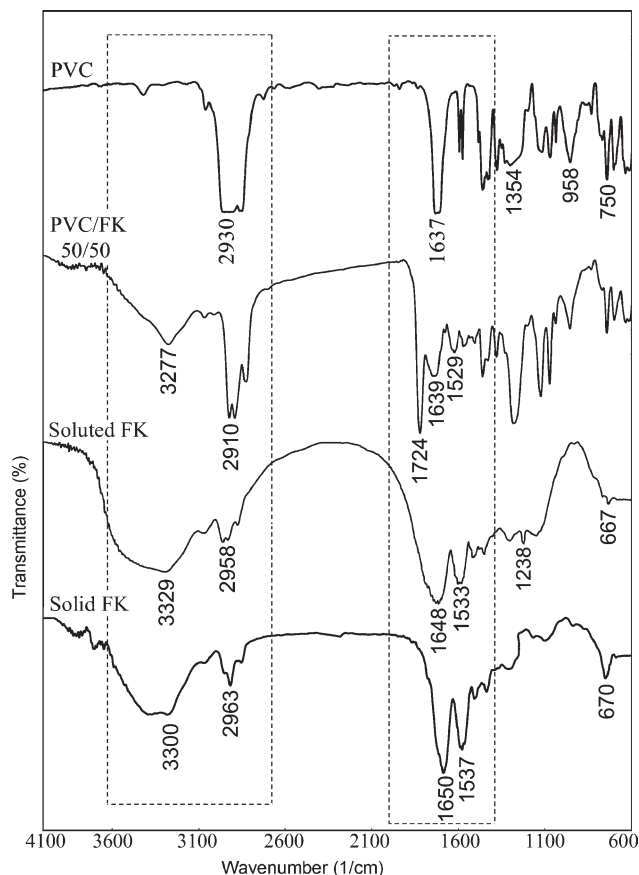


**Figure 4** FTIR spectra of the solid FK, soluted FK, PVC, and PVC/FK 50/50.



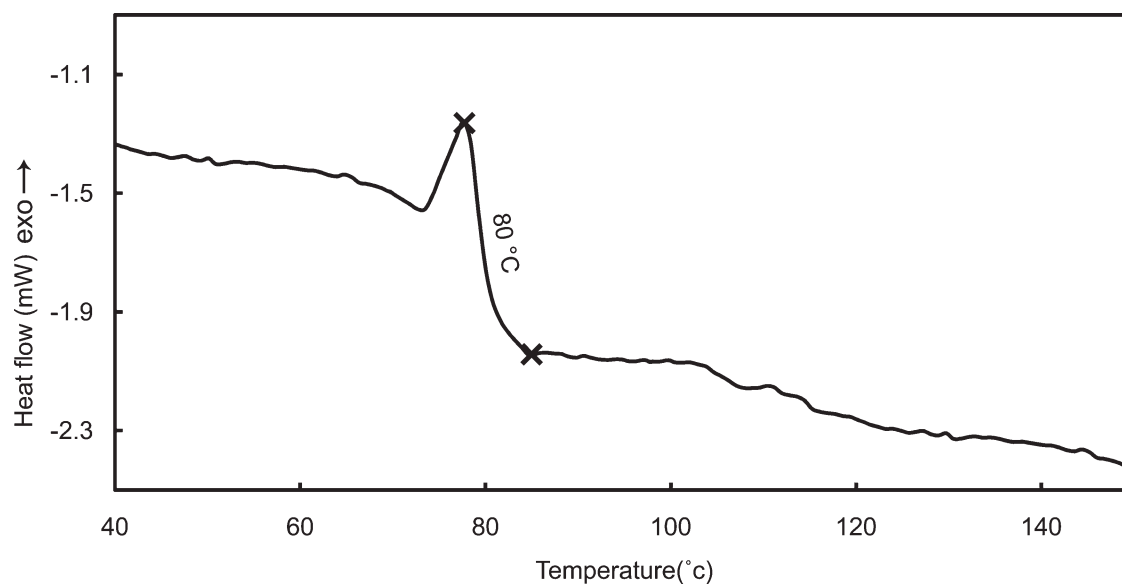**Figure 3** Chemical structures of the most common amino acids in FK.

**Figure 5** DSC curve of the pure PVC.

band), and 2930 cm$^{-1}$ (attributed to C—H vibrations of the C—H—Cl band).[31] In addition, the absorption peak appearing at 1637 cm$^{-1}$ in the neat PVC spectrum corresponded to dioctyl phthalate, commonly used as a plasticizer for PVC.[32]

The observed shifts in the peak positions of both the N—H, C=O and C—H—Cl bands in PVC/FK 50/50 could be attributed to a specific interaction between FK and PVC. Also, a new peak appearing at 1724 cm$^{-1}$ in the PVC/FK 50/50 spectrum was ascribed to the formation of carbonyl groups related to chloroketone. This feature implied that the miscibility of the PVC/FK blend, as revealed by DSV, was due to the hydrogen bonding between the carbonyl groups of FK and hydrogen atoms attached to the chlorine-containing carbons of PVC.[33]

Furthermore, the medium-strong intensity peak at 2963 cm$^{-1}$, ascribed to the FK methyl (CH$_3$) groups' vibrations,[30] shifted to 2910 cm$^{-1}$ in PVC/FK 50/50. According to Schmidt et al.,[34] the changes in the CH$_3$ groups' stretching frequencies in polymers containing water, such as FK,[13] can be related to the amount of water molecules surrounding these CH$_3$ groups in the polymer structure. In other words, the lower the number of water molecules is in interaction with CH$_3$ groups, the larger the wave-number downshifts are on the CH$_3$ vibration.[34] Therefore, we concluded that PVC addition to the FK decreased the water molecules within the FK structure. It is worth mentioning that there was no reduction in the CH$_3$ band absorbance in the soluted FK spectrum compared to that of the solid FK; this suggests that the FK molecular weight remained unchanged during the FK dissolution in DMF.

The DSC curve of the PVC is shown in Figure 5. The $T_g$ value was found to be around 80°C in accord-ance with reports in the literature.[35,36] Also, Figure 6 shows the DSC curves of the pure FK and various PVC/FK blends. The low-temperature peak around
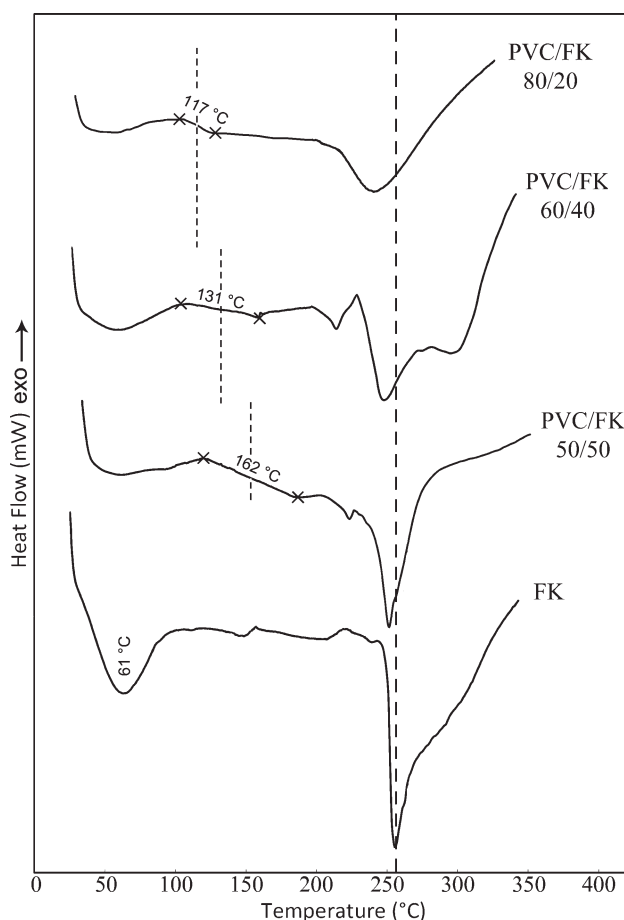


**Figure 6** DSC curves of the pure FK and its various blends with PVC (the curves were shifted vertically for clarity).

### TABLE II
### $T_g$, $T_m$, and $\Delta H_f$ of Pure FK and PVC and Their Various Blends

| Sample | $T_g$ (°C) | $T_m$ (°C) | $\Delta H_m$ (J/g) |
|---|---|---|---|
| FK | — | 258 | 11.86 |
| PVC/FK 50/50 | 162 | 251 | 19.31 |
| PVC/FK 60/40 | 131 | 243 | 31.44 |
| PVC/FK 80/20 | 117 | 238 | 49.54 |
| PVC | 80 | — | — |

60°C in the pure FK DSC curve corresponded to a loss of the so-called chemically bound water or nonfreezing water, which was related to several water layers placed between the FK polypeptidic chains.[37] These free water molecules, which contributed to the conformational stability of the FK, did not have the common water properties and froze at higher temperatures than bulk water.[38] However, the peak mentioned previously disappeared in the PVC/FK blend thermograms. This finding, along with the observation of only one $T_g$ on the thermograms of all the blend samples (Fig. 6), lent credence to the hypothesis that PVC chains entered the amorphous region between the two FK crystallites and confirmed the miscibility of the PVC/FK system. It seemed that the entered PVC chains created new hydrogen bonds with appropriate FK chemical groups, which in turn, led to the decrement of water molecules in the FK structure, as discussed earlier on the basis of FTIR findings. On the other hand, the observed high-temperature transitions in the pure FK and the blends' DSC curves could be attributed to the melting of the FK crystals.[13,28,39]

The most interesting point concerning the results obtained from DSC measurements was the shift of the $T_g$ values of the PVC and the blends under influence of the FK. Table II shows that the PVC $T_g$ was increased by the addition of the FK. The observed increase in the $T_g$ values could have been related to the interactions between the PVC and FK components, which impeded the PVC chain mobility and caused the glass transition to occur at higher temperatures. Furthermore, $T_m$ and $\Delta H_f$ of the FK gradually decreased with the addition of the PVC (Table II). These features are typical characteristics of miscible blends, in which $T_m$ and $\Delta H_f$ of the crystalline component are usually lowered with respect to the pure polymer because of both the diluent effect of the noncrystallizable component and exothermic interaction between the crystalline and amorphous polymers.[40,41]

Figure 7 illustrates the measured values of the blend solutions' refractive indices as a function of their FK content. On the basis of the results reported by various researchers,[42–46] a linear relationship between a blend refractive index and composition can be regarded as a criterion for the blend miscibility. On the other hand,

immiscible blends are expected to present a sigmoidal type curve with two plateaus. As can be observed from Figure 7, these blends' refractive indices obviously had a linear relationship with the FK content ($R^2 = 0.987$). Therefore, we conclude here that the PVC/FK blends were miscible over the studied compositions as well. It is interesting to note that refractometry, which is a simple, low-cost, and rapid method in comparison with viscometry, DSC, and FTIR, could be used as a preliminary test to give an overall view of the polymer blends' miscibility.

Representative AFM height and phase images of PVC/FK 60/40 and PVC/FK 80/20 blends are shown in Figures 8 and 9. Tapping-mode AFM applied here had the advantage of being nondestructive to the polymer film surface compared to contact-mode AFM.[46] Furthermore, tapping-mode AFM is sensitive enough to detect small modulus differences between two phases in a blend film and, hence, can be used to investigate the blends' phase behavior.[46,47] Therefore, the miscibility of the PVC/FK blends was also evaluated on the basis of their AFM phase and height images (Figs. 8 and 9). As can be observed from Figure 8(A,C), FK discreet phases (dark spots) were quite regularly distributed in the continuous PVC phase. Also, in Figure 9(A,C), bright spots of FK are regularly distributed in the PVC matrix. Quantitatively, the dispersed phase domain sizes could be estimated on the basis of the AFM height image.[48] The FK domain sizes were measured as 43.8 and 59.8 nm in the PVC/FK 60/40 and PVC/FK 80/20 blends, respectively. Therefore, similar to the conclusions drawn by Stephens et al.[47] during their studies on polyethylene blends, in both the PVC/FK 60/40 and PVC/FK 80/20 blends, the dispersed phases were distributed molecularly (in nanometer scales) within the matrix phases, and the blends could be regarded as miscible. Also, the mean horizontal distances between the PVC and FK phases increased from 32 to 264 nm, and the mean vertical distances increased from 180 to 286 nm in the PVC/FK 60/40 and PVC/FK 80/20 blends, respectively. Accordingly, the markedly reduced FK domain size and PVC and FK phase distances in the
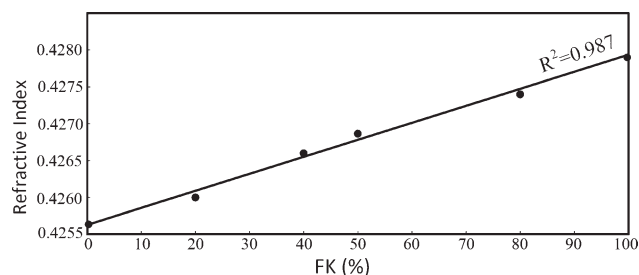


**Figure 7** PVC/FK solutions' refractive indices as a function of FK content.
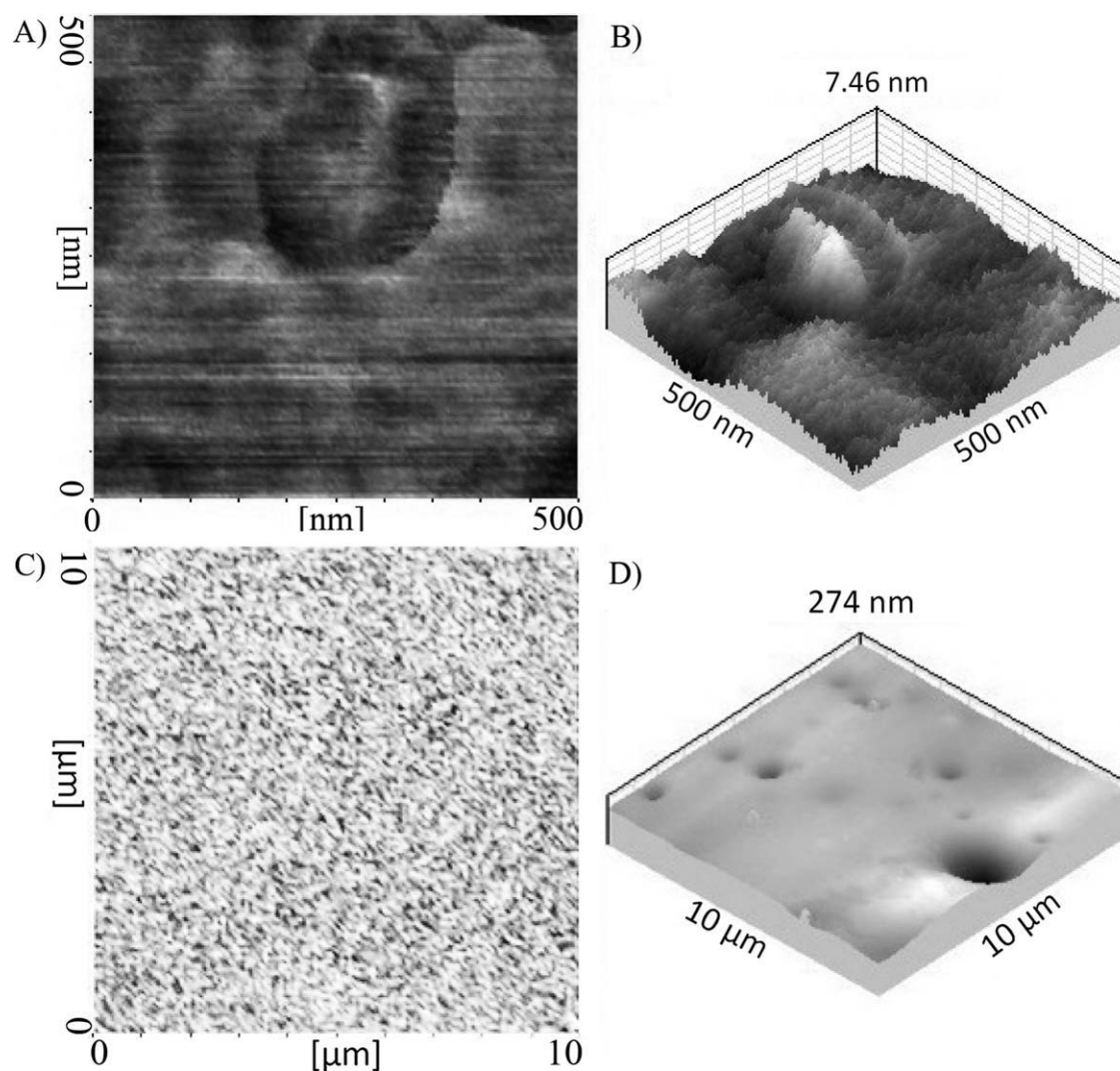
**Figure 8** AFM image of the PVC/FK 60/40 blend: (A) 500-nm phase image, (B) 500-nm height image, (C) 10-μm phase image, and (D) 10-μm height image.

PVC/FK 60/40 blend could be attributed to their enhanced miscibility degree;[49] this was in accordance with our previous findings in this work. Furthermore, the texture in the height images of the PVC/FK 60/40 [Fig. 8(B,D)], which was caused by surface roughness,[47] was smoother than that of the PVC/FK 80/20 blend [Fig. 9(B,D)]; this, again, pointed to the higher degree of miscibility in the former. Upon close examination of the PVC/FK 60/40 blend AFM image (Fig. 8), one can observe a nanophase separation within the domains, indicated by the FK phase with the dark contrast within the brighter PVC domains. However, the colors of the dispersed and matrix phases appeared to be changed in the PVC/FK 80/20 blend image (Fig. 9). According to Raghavan et al.,[48] this color flipping may be related to the competition between AFM tip–sample attractive and repulsive interaction forces. As was shown earlier, FK has many polar groups (Fig. 3), whereas PVC is essentially nonpolar in nature.

Hence, the flip in phase contrast from the PVC/FK 60/40 blend, containing 40 wt % of the polar component, to PVC/FK 80/20, including 80 wt % of the nonpolar component, was caused by the switch from the tip–sample attractive interaction to repulsive interaction, respectively.

In addition, because of the crucial role of thermal stability in the final performance of the biobased polymer blends, the thermal behavior of the prepared samples was investigated by TGA. Figures 10 and 11 show the differential thermogravimetry (DTG) and TGA curves of pure PVC, FK, and their different blends, respectively. Pure FK revealed a weight loss in three stages, which appeared as three distinct peaks in its DTG curve (Fig. 10). The first stage in the low-temperature range was due to the removal of its structural water. On the other hand, the second one, between 250 and 280°C, was related to the FK helix structure degradation followed by the thermal pyrolysis of peptide bridges. The third peak, around 300°C, was
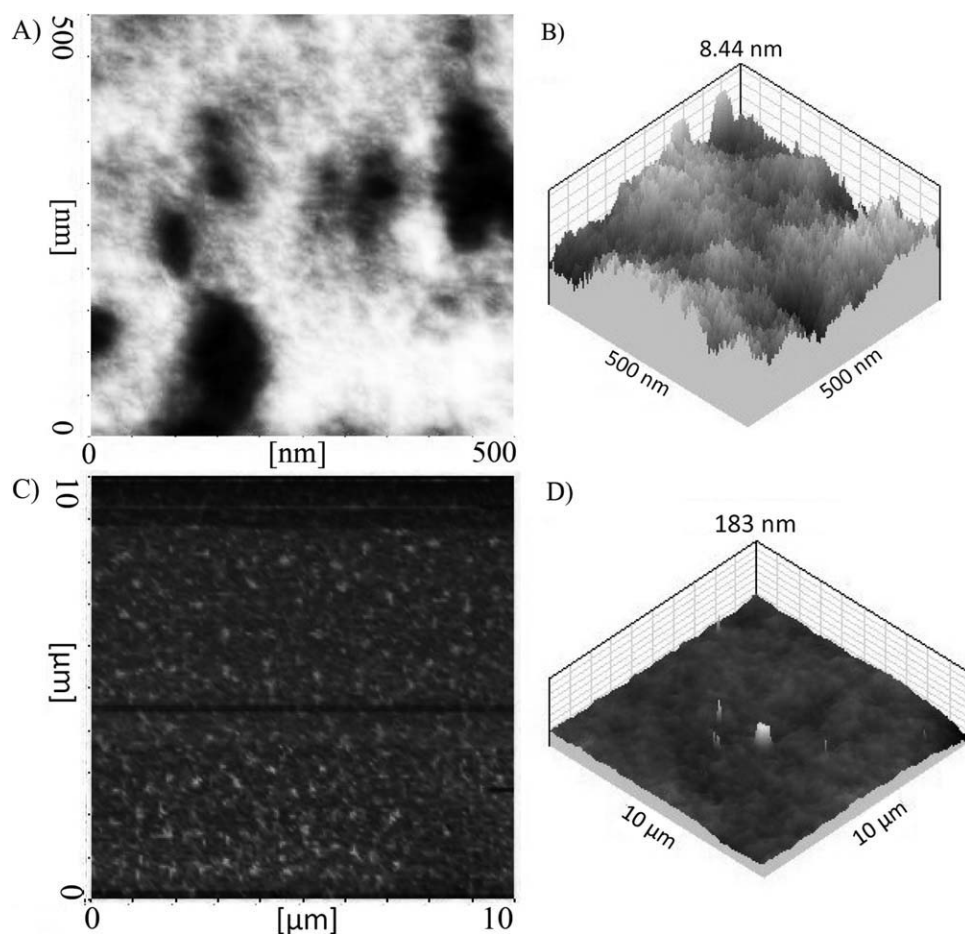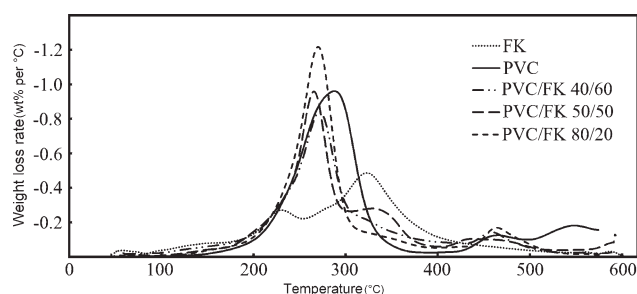
**Figure 9**   AFM image of the PVC/FK 80/20 blend: (A) 500-nm phase image, (B) 500-nm height image, (C)10-µm phase image, and (D) 10-µm height image.

attributed to the FK backbone cleavage and final decomposition.[37] Also, the one-step degradation of PVC (Fig. 10) was a result of its side-group elimination followed by main-chain scissioning.[50]

The thermal behavior of the PVC/FK blends can be discussed in two distinct temperature regions. In the temperature range below 250°C, increasing the amount of the PVC component in the blends increased their thermal stabilities, as inferred from the higher onset degradation temperatures of the PVC-rich blends compared to the FK-rich ones.

However, as can be seen from Figure 11, such a trend was not followed in the temperature range above 250°C. Indeed, at temperatures higher than 250°C, increasing the FK content of the blends increased their thermal stabilities. It seemed that the byproducts of the initial thermal degradation of the



**Figure 10**   DTG curves of the pure PVC, FK, and their various blends.
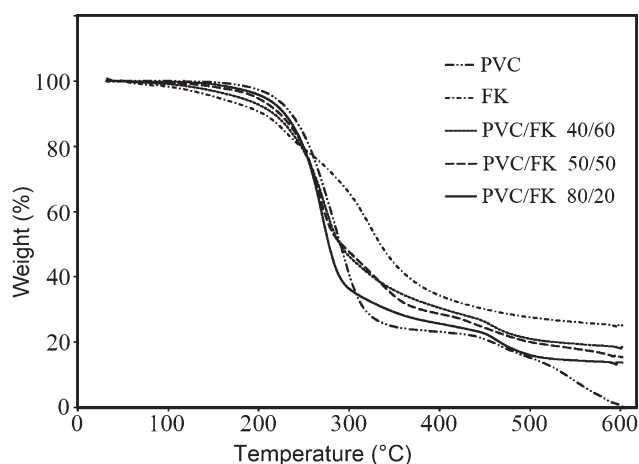


**Figure 11**   TGA curves of the pure PVC, FK, and their various blends.

blends' FK component contributed to the formation of a char layer on the material surface. Such a protective barrier not only impeded the heat transfer to the system but also decelerated the escape of volatile small molecules, such as HCl, $CO_2$, $H_2O$, HCN, and $H_2S$, resulting from the PVC or the remaining FK degradation.[17] Interestingly, this protective mechanism of the FK is similar to nitrogen-containing flame retardants in various systems.[51]

## CONCLUSIONS

In this work, DSV, FTIR spectroscopy, DSC, refractometry, and AFM methods were performed to investigate the miscibility of PVC/FK blends. According to all the aforementioned methods, PVC and FK formed miscible blends. The miscibility was found to be a result of specific interactions between carbonyl groups of the FK structure with hydrogen from CHCl groups of the PVC. Also, it was demonstrated that blends with a higher amount of FK showed a higher degree of miscibility. Furthermore, the efficiency of the simple refractometry method as an alternative for DSV, FTIR spectroscopy, DSC, and AFM methods to investigate the polymer blends miscibility was confirmed. Finally, TGA results show that FK could play a role as a flame retardant for the studied blends. Hopefully, the results of this work can pave the way for subsequent investigations on the design and development of ecofriendly polymeric products.

## References

1. Martelli, S. M.; Moore, G.; Paes, S. S.; Gandolfo, C.; Laurindo, J. B. LWT—Food Sci Technol 2006, 39, 292.
2. Walker, A. M.; Tao, Y.; Torkelson, J. M. Polymer 2007, 48, 1066.
3. Martinez-Hernandez, A. L.; Velasco-Santos, C.; Icaza, M.; Castano, V. M. Compos B 2007, 38, 405.
4. Huda, S.; Yang, Y. J Polym Environ 2009, 17, 131.
5. Bertsch, A.; Coello, N. Bioresour Technol 2005, 96, 1703.
6. Poopathi, S.; Abidha, S. Biol Control 2007, 43, 49.
7. Poopathi, S.; Abidha, S. Int Biodeterior Biodegrad 2008, 62, 479.
8. Schrooyen, P. M. M.; Dijkstra, P. J.; Oberthur, R. C.; Bantjes, A.; FeijenJ. J Agric Food Chem 2000, 48, 4326.
9. Schrooyen, P. M. M.; Dijkstra, P. J.; Oberthur, R. C.; Bantjes, A.; FeijenJ. J Agric Food Chem 2001, 49, 221.
10. Tanabe, T.; Okitsu, N.; Yamauchi, K. Mater Sci Eng C 2004, 24, 441.
11. Fujii, T.; Li, D. J Biol Macromol 2008, 8, 48.
12. Poole, A. J.; Church, J. S.; Huson, M. G. Biomacromolecules 2009, 10, 1.
13. Barone, J. R.; Schmidt, W. F. Compos Sci Technol 2005, 65, 173.
14. Barone, J. R. Compos A 2005, 36, 1518.
15. Huda, S.; Yang, Y. Compos Sci Technol 2008, 68, 790.
16. Martinez-Hernandez, A. L.; Velasco-Santos, C.; Icaza, M.; Castano, V. M. Polymer 2005, 48, 8233.
17. Cheng, S.; Lau, K.; Liu, T.; Zhao, Y.; Lam, P.; Yin, Y. Compos B 2009, 40, 650.
18. Mishra, S. C.; Nayak, N. B.; Satapathy, A. J Reinf Plast Compos 2009, 25, 1.
19. Barone, J. R.; Gregoire, N. T. Compos Plast Rubber Compos 2006, 35, 287.
20. Ye, Y.; Dan, W.; Zeng, R.; Lin, H.; Dan, N.; Guan, L. Eur Polym J 2007, 43, 2066.
21. Krigbaum, W. R.; Wall, F. W. J Polym Sci 1950, 5, 505.
22. Cragg, L. H.; Bigelow, C. C. J Polym Sci 1955, 16, 177.
23. Williamson, G.; Wright, R. J Polym Sci 1965, 3, 3885.
24. Chee, K. K. Eur Polym J 1990, 26, 423.
25. Garcia, R.; Melad, O.; Gomez, C. M.; Figueruelo, J. E.; Campos, A. Eur Polym J 1999, 35, 47.
26. Lizymol, P. P.; Thomas, S. J Appl Polym Sci 1994, 51, 635.
27. Walsh, D. J.; Higgins, J. S.; Rostami, S. Macromolecules 1983, 16, 388.
28. Martinez-Hernandez, A. L.; Velasco-Santos, C.; Icaza, M.; Castano, V. M. Int J Environ Pollut 2005, 23, 162.
29. Akhtar, W.; Edwards, H. G. M. Spectrochim Acta Part A 1997, 53, 81.
30. Barone, J. R.; Arikan, O. Polym Degrad Stab 2007, 92, 859.
31. Rajendran, S.; Prabhu, M. R.; Rani, M. U. Int J Electrochem Sci 2008, 3, 282.
32. Monteiro, S. S. A.; Fernanda, P. M.; Raimundo, I. M.; Almeida, Y. M. B. Sens Actuators B 2009, 139, 222.
33. Khan, M. S.; Qazi, R. A.; Wahid, M. S. Afr J Pure Appl Chem 2008, 2, 41.
34. Schmidt, P.; Dybal, J.; Trchova, M. Vib Spectrosc 2006, 42, 278.
35. Ramesh, S.; Yi, L. J. Ionics 2009, 15, 282.
36. Ramesh, S.; Liew, C. W.; Morris, E.; Durairaj, R. Thermochim Acta 2010, 511, 140.
37. Verbeek, C. J. R.; Van Den Berg, L. E. Macromol Mater Eng 2010, 295, 10.
38. Hatakeyama, H.; Hatakeyama, T. Thermochim Acta 1998, 308, 3.
39. Barone, J. R.; Dangaran, K. W.; Schimidt, F. J Agric Food Chem 2006, 54, 5393.
40. Lewandowska, K. Eur Polym J 2005, 41, 55.
41. Kim, G. S.; Son, J. M.; Lee, J. K.; Lee, K. H. Eur Polym J 2010, 46, 1696.
42. Rajulu, A. V.; Reddy, R. L.; Raghavendra, S. M.; Akheel Ahmed, S. Eur Polym J 1999, 35, 1183.
43. Basavaraju, K. C.; Jayaraju, J.; Rai, S. K.; Damappa, T. J Appl Polym Sci 2008, 109, 2491.
44. Qiu, Z.; Ikehara, T.; Nishi, T. Polymer 2003, 44, 2503.
45. Ramswamy Illiger, S.; Fadnis, C.; Demappa, T.; Jayaraju, J.; Keshavayya, J. Carbohydr Polym 2009, 75, 484.
46. Antony, P.; Kwon, Y.; Puskas, J. E.; Kovar, M.; Norton, P. R. Eur Polym J 2004, 40, 149.
47. Stephens, C. H.; Hiltner, A.; Baer, E. Macromolecules 2003, 36, 2733.
48. Raghavan, D.; Van Landingham, M.; Gu, X.; Nguyen, T. Langmuir 2000, 16, 9448.
49. Cho, Y. G.; Kamal, M. R. Polym Eng Sci 2005, 42, 2005.
50. Menczel, J. D.; Bruce, P. R. Thermal Analysis of Polymer; Wiley: Hoboken, NJ, 2009; p 261.
51. Lu, S.; Hamerton, I. Prog Polym Sci 2002, 27, 1661.